The relaxation of OH ($v = 1$) and OD ($v = 1$) by H_2O and D_2O at temperatures from 251 to 390 K

D. C. McCabe,†[abc] B. Rajakumar,‡[ac] P. Marshall,[d] I. W. M. Smith[e] and
A. R. Ravishankara[abc]

We report rate coefficients for the relaxation of OH($v = 1$) and OD($v = 1$) by H_2O and D_2O as a function of temperature between 251 and 390 K. All four rate coefficients exhibit a negative dependence on temperature. In Arrhenius form, the rate coefficients for relaxation (in units of 10^{-12} cm^3 molecule^{-1} s^{-1}) can be expressed as: for OH($v = 1$) + H_2O between 263 and 390 K: $k = (2.4 \pm 0.9) \exp((460 \pm 115)/T)$; for OH($v = 1$) + D_2O between 256 and 371 K: $k = (0.49 \pm 0.16) \exp((610 \pm 90)/T)$; for OD($v = 1$) + H_2O between 251 and 371 K: $k = (0.92 \pm 0.16) \exp((485 \pm 48)/T)$; for OD($v = 1$) + D_2O between 253 and 366 K: $k = (2.57 \pm 0.09) \exp((342 \pm 10)/T)$. Rate coefficients at ($297 \pm 1$ K) are also reported for the relaxation of OH($v = 2$) by D_2O and the relaxation of OD($v = 2$) by H_2O and D_2O. The results are discussed in terms of a mechanism involving the formation of hydrogen-bonded complexes in which intramolecular vibrational energy redistribution can occur at rates competitive with re-dissociation to the initial collision partners in their original vibrational states. New *ab initio* calculations on the H_2O–HO system have been performed which, *inter alia*, yield vibrational frequencies for all four complexes: H_2O–HO, D_2O–HO, H_2O–DO and D_2O–DO. These data are then employed, adapting a formalism due to Troe (J. Troe, *J. Chem. Phys.*, 1977, **66**, 4758), in order to estimate the rates of intramolecular energy transfer from the OH (OD) vibration to other modes in the complexes in order to explain the measured relaxation rates—assuming that relaxation proceeds *via* the hydrogen-bonded complexes.

1. Introduction

The notion that vibrational energy transfer in molecular collisions is facilitated by the presence of strong attraction between the collision partners is one of long-standing.[1] The most clear cut examples of this effect are when the collision partners form a chemical bond. Examples include the relaxation of NO($v = 1$) by O and Cl atoms,[2] and of OH($v = 1$), OD($v = 1$) and OH($v > 0$) by NO$_2$,[3,4] of OH($v = 1$), OD($v = 1$) by NO,[3] of OH($v = 1$), OD($v = 1$) by CO,[5] and of OH($v = 1$) by SO$_2$.[6] The large magnitude of the rate coefficients for these processes and the similarity of the rate coefficients for the

relaxation of OH($v = 1$) and OD($v = 1$) by the same species are rather clear indications that relaxation occurs *via* complex-forming collisions, since the large difference in the vibrational transition energies in OH and OD will dramatically change the probability of vibration-to-vibration (V–V) energy exchange.[1] In these instances of strong intermolecular forces, it appears that intramolecular vibrational energy redistribution (IVR) in the initially formed complex is rapid relative to re-dissociation to the collision partners in their original vibrational states, so that the rate constant for relaxation corresponds to that for initial association of the two species. Such measurements then provide an estimate of the rate coefficient for the association reaction of the same two species in the limit of high pressure.[7] It is anticipated that the rate constants for both these processes (relaxation and high pressure association) will show a negative, but only a mild negative, dependence on temperature.

The role in vibrational energy transfer of molecular attractions of intermediate strength, specifically those arising from hydrogen bonds, has long been debated. In particular, such forces were invoked in the 1970s to explain the rapid rates observed for the vibrational relaxation of HF($v = 1$) both in HF–HF collisions[8,9] and in collisions with H_2O.[8b,9–11] In such cases, it is less likely that IVR in any complex that is formed will occur faster than re-dissociation to the collision partners in their original vibrational states. Consequently, the mechanism for vibrational relaxation must take account of the competition between IVR in the complex and its re-dissociation without

[a] NOAA Aeronomy Laboratory, 325 Broadway R/AL2, Boulder, Colorado, 80305, USA
[b] Department of Chemistry and Biochemistry, University of Colorado, Boulder, Colorado, 80309, USA
[c] CIRES, University of Colorado, 80309, USA. E-mail: ravi@al.noaa.gov
[d] Department of Chemistry and Center for Advanced Scientific Computing and Modeling, University of North Texas, PO Box 305070, Denton, Texas, 76203-5070, USA. E-mail: marshall@unt.edu
[e] The University Chemical Laboratory, Lensfield Road, Cambridge, UK CB2 1EW. E-mail: i.w.m.smith@bham.ac.uk or iwms2@cam.ac.uk
† Present address: Division of Engineering and Applied Sciences, California Institute of Technology, Pasadena, CA 91125, USA. E-mail: dmcc@caltech.edu
‡ Present address: Department of Chemistry, Indian Institute of Technology, Madras 600 036, India. E-mail: rajakumar@iitm.ac.in.

Table 1 Predicted dissociation energies (D_0/kJ mol^{-1}) and bonding enthalpies ($\Delta_r H^0_{298}$/kJ mol^{-1}) of OH–H$_2$O complexes

H$_2$O–HO $^2A'$		H$_2$O–HO $^2A''$		HOH–OH $^2A''$		
D_0/kJ mol^{-1}	$\Delta_r H^0_{298}$/kJ mol^{-1}	D_0/kJ mol^{-1}	$\Delta_r H^0_{298}$/kJ mol^{-1}	D_0/kJ mol^{-1}	$\Delta_r H^0_{298}$/kJ mol^{-1}	Ref.
	$-(17.2\text{–}18.0)$				$-(8.8\text{–}9.6)$	18e
15.7^a	-9.9^{bc}	13.9^a	-6.9^{bc}	9.0^a	-4.7^{bc}	18f,h
21.3–23.8						18d
					-8.8	18b
17.6–18.0^d	$-(20.5\text{–}20.9)^b$				-10.9^b	18a
15.5^a	-18.0^a	$D_e = 22.2$		$D_e = 14.6$		18g
				$D_e = 14.6$		18c

^{a} As calculated using the reported value for D_e and the reported vibrational frequencies. ^{b} As calculated using the reported value of $\Delta_r E^0_{298}$ ($\Delta_r H^0_{298} = \Delta_r E^0_{298} - RT$ since one mole of gas is lost in the reaction). ^{c} Based on the reported D_e and vibrational frequencies, the value of $\Delta_r E^0_{298}$ these authors reported appears to be erroneous; the value of $\Delta_r H^0_{298}$ listed here is based on their reported $\Delta_r E^0_{298}$. ^{d} As calculated using the reported values of D_e and by reproducing the reported electronic structure calculation to retrieve the predicted frequencies.

loss of the initial vibrational excitation. This mechanism is akin to that for collisionally stabilised association, with IVR taking the place of collisional stabilisation. In the limit where IVR is much slower than re-dissociation, one would expect a rather strong negative temperature-dependence of the relaxation rate constant, as for association reactions in the low pressure limit.[7] Once again, comparisons of rate constants for hydrogenated and deuterated species, as well as measurements of the temperature-dependence of the relaxation rate, can provide useful information by altering the energy discrepancies for any V–V relaxation channels.
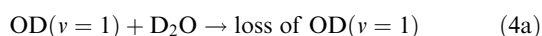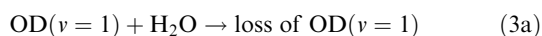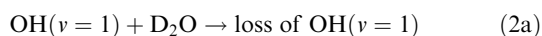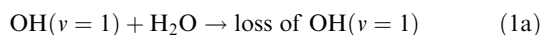
Recently, we reported a rather extensive study of the relaxation of OH($v = 1$) and OD($v = 1$) by HNO$_3$ and DNO$_3$.[12] Rate coefficients for removal of the vibrationally excited radicals were measured for all four pairs of colliders in the temperature range from 253 to 383 K. All four rate coefficients exhibit a fairly strong negative dependence on temperature. It was concluded that removal of the vibrationally excited OH (OD) radicals occurs via the formation of hydrogen-bonded cyclic complexes that had previously been invoked[13] to explain the unusual temperature- and pressure-dependence of the rate constant for the chemical reaction of OH($v = 0$) with HNO$_3$. However, in contrast to the systems where a strong chemical bond forms between the collision partners, in this case it was proposed that IVR and re-dissociation without loss of vibrational excitation in the OH (OD) radical occurred at comparable rates, so that the rate coefficients for relaxation were less than those for formation of the energised complex.

In the present paper, we report the results of a similar investigation to that on the OH($v = 1$), OD($v = 1$) + HNO$_3$, DNO$_3$ system; this time on the relaxation of OH($v = 1$) and OD($v = 1$) by H$_2$O and by D$_2$O. Recently, there have been two reports[14,15] of the observation of the H$_2$O–HO hydrogen-bonded species by gas-phase rotational spectroscopy. In addition, there have been two reports[16] of the infrared spectrum of H$_2$O−HO in solid argon matrices, as well as investigations[17] of the potential energy surface for H$_2$O−HO using photoelectron spectroscopy. However, there has been no experimental determination of the dissociation energy of the hydrogen-bonded complex.
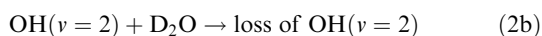
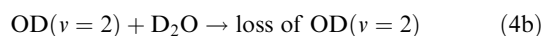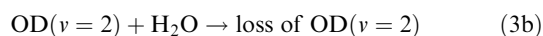There have also been several theoretical studies[18,19] of the H$_2$O–HO and HOH–OH hydrogen-bonded complexes. The dissociation energies (D_0) and bond enthalpies ($\Delta_r H^0_{298}$) suggested by these studies are summarised in Table 1. Several minima have been located on the potential energy surface. The consensus view (for example, ref. 18g) is that the lowest minimum is associated with a structure of $^2A'$ symmetry in which the OH radical acts as the proton donor and the water molecule the proton acceptor (which we shall refer to as H$_2$O–HO), with a slightly weaker bond associated with the $^2A''$ complex in which the roles are reversed; i.e., H$_2$O is the proton donor and OH the proton acceptor (which we shall refer to as HOH–OH). In part, these theoretical studies focus on the path and energy barrier for the isotopic exchange reaction, HO + H'OH'' → HOH' + OH''. Masgrau et al.[18d] concluded that this reaction proceeds via formation of the hydrogen-bonded H$_2$O–HO species followed by tunnelling through a substantial barrier to form the products. In addition, they estimated a rate constant for association to this complex of 3.7×10^{-10} cm^3 molecule^{-1} s^{-1}.

In the present work, rate coefficients for vibrational relaxation were measured using pulsed laser photolysis (PLP) to generate vibrationally excited OH (OD) and pulsed laser-induced fluorescence (PLIF) to detect the vibrationally excited radicals. This technique is quite similar to that which we employed to measure the rate coefficients for vibration relaxation of OH($v = 1$) and OD($v = 1$) by HNO$_3$ and DNO$_3$.[12] Using this method, we have measured rate coefficients, at temperatures between 251 and 390 K, for the following processes:

$$\text{OH}(v = 1) + \text{H}_2\text{O} \rightarrow \text{loss of OH}(v = 1) \quad (1a)$$

$$\text{OH}(v = 1) + \text{D}_2\text{O} \rightarrow \text{loss of OH}(v = 1) \quad (2a)$$

$$\text{OD}(v = 1) + \text{H}_2\text{O} \rightarrow \text{loss of OD}(v = 1) \quad (3a)$$

$$\text{OD}(v = 1) + \text{D}_2\text{O} \rightarrow \text{loss of OD}(v = 1) \quad (4a)$$

In general, the photochemistries that were used to produce OH($v = 1$) and OD($v = 1$) also produce significant amounts of the radicals in the ($v = 2$) vibrational state. We took advantage of this to measure the previously unreported rate coefficients at ca. 298 K for the following relaxation processes:

$$\text{OH}(v = 2) + \text{D}_2\text{O} \rightarrow \text{loss of OH}(v = 2) \quad (2b)$$

$$OD(v = 2) + H_2O \rightarrow loss\ of\ OD(v = 2) \qquad (3b)$$

$$OD(v = 2) + D_2O \rightarrow loss\ of\ OD(v = 2) \qquad (4b)$$

2. Experimental details

Rate coefficients for the processes represented by eqns (1) to (4) were measured using pulsed laser photolytic methods to produce $OH(v > 0)$ or $OD(v > 0)$ and pulsed LIF to detect OH or OD radicals in specific vibrational levels. Gas mixtures, containing the species required to create the vibrationally excited radicals and H_2O or D_2O, were diluted to total pressures in the range 22 to 34 Torr with helium and flowed slowly through the reaction cell. The excess of He ensured complete translational and rotational equilibration of species, on a time scale much shorter than that associated with the kinetic observations that we report, but did not cause significant quenching of the LIF signals. The flow rate was fast enough to ensure that a fresh sample of gas mixture was exposed to successive shots from the photolysis laser. The apparatus which was employed in the present study has been used in numerous previous kinetic studies, including that in which rate coefficients were measured for the relaxation of $OH(v = 1)$ and $OD(v = 1)$ by HNO_3 and DNO_3,[12] and it is described in detail elsewhere.[20] Here we focus on those aspects of our experimental procedure that were required for the present measurements.

Since it is not straightforward to generate vibrationally excited OH (OD) radicals by direct photolysis of H_2O (D_2O), it was necessary to include other photolytes in the gas mixtures; these are listed in Table 2. For measurements on process (1a), the relaxation of $OH(v = 1)$ by H_2O, three different schemes were used to generate $OH(v = 1)$: (i) the direct photolysis of HNO_3; (ii) the direct photolysis of H_2O_2; and (iii) the reaction between $O(^1D)$ atoms, produced from ozone photolysis, and H_2O. In all cases, photolysis was performed with the 248 nm output of an excimer laser operating on KrF. The excimer laser beam (ca. 20–80 mJ per pulse and with a cross-sectional area of ca. 1.5 cm^2) was directed perpendicular to the gas flow. Photolysis of HNO_3 at

Table 2 Source chemistry for production of vibrationally excited OH/OD

Process studied	Photolyte(s)	Species[a] reacting with $O(^1D)$	Maximum v level accessible
$OH(v = 1) + H_2O$	HNO_3, H_2O_2		7, 7[b]
$OH(v = 1) + H_2O$	O_3	H_2O	3
$OH(v = 1, 2) + D_2O$	O_3	CH_4	4
$OD(v = 1, 2) + H_2O$	O_3	CD_4	6
$OD(v = 1, 2) + D_2O$	O_3	D_2O	4

[a] Species which reacts with $O(^1D)$ to produce vibrationally excited OH (OD). [b] Although these are the highest levels accessible energetically from photodissociation at 248 nm, the yield of $OH(v > 0)$ is small from both these photodissociations. The highest vibrational levels that have been observed to be populated are $v = 2$ from HNO_3 and $v = 1$ from H_2O_2. There is further discussion in the text.

248 nm is known to generate a small fraction (ca. 1%) of OH in $v = 1$, roughly half that amount in $v = 2$, and little or none in higher vibrational levels.[12] The yield of $OH(v = 1)$ from photolysis of H_2O_2 at 248 nm is reported[21] to be less than 1%. Evidence from our own work indicates that the yield in higher vibrational levels is negligible. Moreover, using this source, the $OH(v = 1)$ LIF signal levels were quite low, indicating that the relative yield of $OH(v = 1)$ is significantly smaller from the photolysis of H_2O_2 than it is from HNO_3.

In experiments on the relaxation of $OH(v)$ by D_2O and of $OD(v)$ by H_2O and D_2O, reactions of $O(^1D)$ were used to generate the vibrationally excited radicals, as indicated in Table 2. The reactions of $O(^1D)$ with H_2O, D_2O, CH_4, and CD_4 all produce vibrationally excited OH or OD in significant yields. Furthermore, the photolysis cross section of O_3 and the quantum yield for production of $O(^1D)$ at 248 nm are both large. These factors combine to allow significant production of vibrationally excited OH or OD while using relatively small concentrations of photolytic precursors. This is important because species such as H_2O, D_2O, HNO_3, DNO_3, and, to a lesser extent, CH_4 and CD_4, efficiently quench the electronically excited $A^2\Sigma^+$ state of OH (OD) which is excited during the LIF detection of vibrationally excited OH (OD) in our experiments. CH_4 and CD_4, instead of H_2O and D_2O, were used as precursors of vibrationally excited OH and OD for measurements of processes (2) and (3) primarily because CH_4 (CD_4) electronically quenches $A^2\Sigma^+$ OH (OD) less efficiently than H_2O (D_2O).

With the exception of H_2O_2 photolysis, all of the sources of $OH(v = 1)$ and $OD(v = 1)$ produce the radicals in vibrational states above $v = 1$. Table 2 shows the highest thermodynamically accessible vibrational state for the OH (OD) product of the $O(^1D)$ reactions that we used. (For $O(^1D) + H_2O$, a small yield of $OH(v = 3)$ is observed,[22] although this reaction is slightly endothermic.) Previous work has shown that the yield of $OH(v \geq 2)$ is significant for $O(^1D) + H_2O$[23] and $O(^1D) + CH_4$,[24] and that the yield of OD ($v \geq 2$) is significant from $O(^1D) + D_2O$.[25] We are not aware of any reports of the yield of $OD(v \geq 1)$ from $O(^1D) + CD_4$, but we observed that significant OD is produced in at least $v = 1, 2, 3$.

The presence of OH or OD in levels above $v = 1$ presents a significant complication in our measurements of rate coefficients for the relaxation of $OH(v = 1)$ and $OD(v = 1)$, because radicals in these higher vibrational states are relaxed into ($v = 1$) as the population in that level is being simultaneously removed. Thus, the temporal profiles for the vibrationally excited radicals are not single-exponential decays. The analysis of these temporal profiles is discussed in the next section.

Vibrationally excited OH (OD) radicals were observed using LIF. The second harmonic of a tuneable dye laser pumped by the second harmonic of a pulsed Nd:YAG laser ($\lambda = 532$ nm) was passed through the reaction cell, perpendicular to both the gas flow and the photolysis laser. This probe laser excited a specific rotational line in the $A^2\Sigma^+$ ($v = 0$) $\leftarrow$ $X^2\Pi$ ($v = 1$) band of OH or OD, in order to detect $OH(v = 1)$ or $OD(v = 1)$, or in the $A^2\Sigma^+$ ($v = 1$) $\leftarrow$ $X^2\Pi(v = 2)$ band, to detect $OH(v = 2)$ or $OD(v = 2)$. The $Q_1(1)$ lines in these bands were used, except for measurements on $OD(v = 2)$. In this case the $Q_1(1)$ line could not be used because it is too close in

This journal is © the Owner Societies 2006

Phys. Chem. Chem. Phys., 2006, **8**, 4563–4574 | 4565

wavelength to several OD $A^2\Sigma^+(v = 0) \leftarrow X^2\Pi (v = 1)$ transitions. The wavelength used for OD($v = 2$) excited both the $R_2(1)$ and $P_1(4)$ lines.

OH (OD) $A^2\Sigma^+ \rightarrow X^2\Pi$ fluorescence passed through a band-pass filter (peak transmission at 307.5 nm, FWHM 10 nm) and was detected with a photomultiplier tube (PMT) positioned orthogonally to the laser beams. When OH (OD) $X^2\Pi(v = 1)$ was excited to $A^2\Sigma^+ (v = 0)$, emission in the $A^2\Sigma^+ (v = 0) \rightarrow X^2\Pi(v = 0)$ band ($\lambda \approx 308$ nm for both OH and OD) was transmitted by the band-pass filter and detected. When OH (OD) $X^2\Pi(v = 2)$ was excited to $A^2\Sigma^+(v = 1)$, emission from two bands was detected: directly excited emission in the (1,1) band ($\lambda \approx 313$ nm for OH, 311 nm for OD), and, after vibrational relaxation of OH (OD) $A^2\Sigma^+(v = 1)$, emissions in the (0,0) band. Temporal profiles of the LIF signals were generated by varying the time delay between the pulses from the photolysis and probe lasers.

The LIF detection scheme that was adopted had several advantages. Because the excitation wavelengths (in the range 334–351 nm) were longer than those of the LIF signals (at *ca.* 308 nm) any scattered light would have to have been blue shifted to be detected. Furthermore, species such as HNO$_3$ and O$_3$ have negligible photolysis cross sections at the excitation wavelengths, so the probe laser did not produce significant amounts of OH($v = 1$) or OD($v = 1$).

H$_2$O or D$_2$O was introduced into the reaction cell by bubbling a small flow of He through either distilled H$_2$O or D$_2$O (Aldrich, 99.9% atom D). The flow from this bubbler, which was at room temperature, was then passed through a second bubbler, which was kept below room temperature (typically 0 °C for H$_2$O and 5 or 10 °C for D$_2$O). We assumed that the flow left the second bubbler saturated with H$_2$O (D$_2$O) at the temperature of that bubbler. The concentration of H$_2$O (D$_2$O) in the reaction cell was calculated using the saturation vapour pressure of H$_2$O[26] or D$_2$O[27] at the temperature of the second bubbler and dilution factors based on the various flows, the temperature of the reaction cell, and the pressures of the second bubbler and the reaction cell. We estimate that the concentration of H$_2$O (D$_2$O) in the reaction cell had an uncertainty of *ca.* 9% associated with an estimated uncertainty of ±0.5 K (2σ) in the temperature of the second bubbler and the uncertainty in the dilution factors. Rate coefficients below room temperature were measured with partial pressures of H$_2$O (D$_2$O) at least three times lower than the saturation vapour pressures of these compounds over solid H$_2$O[28] or D$_2$O[29] at the temperature of the reaction cell.

Anhydrous HNO$_3$ and DNO$_3$ were prepared by vacuum distillation of the nitric acid formed by the addition of H$_2$SO$_4$ or D$_2$SO$_4$ to NaNO$_3$ and stored at reduced temperature in glass bubblers. Gas-phase HNO$_3$ and/or DNO$_3$ was introduced into the gas flow by bubbling a small flow of He through the liquid acid in the bubbler. Gas phase H$_2$O$_2$ was introduced into the system by flowing a small amount of He through a concentrated aqueous solution of hydrogen peroxide (estimated to be >95% by titration with potassium permanganate).

Ozone was prepared by passing ultra-high purity (UHP) O$_2$ through an electrical discharge and then trapping the O$_3$ that was formed on silica gel at *ca.* 197 K. Dilute (*ca.* 200 ppmv) mixtures of O$_3$ in He were then prepared manometrically and stored in darkened 12 l glass bulbs. Methane and per-deuteromethane (UHP grade) were used as supplied. Helium (UHP grade) was also used directly out of its cylinder.

3. Data analysis and estimates of errors

For each of the rate coefficients presented here, with the exception of the measurement of OH($v = 1$) relaxation by H$_2$O when H$_2$O$_2$ was used as the photolyte, temporal profiles of the concentrations of vibrationally excited radicals observed by PLIF were *not* single-exponential. This was due to the presence of higher vibrational states of the OH or OD radical being relaxed into the vibrational state being monitored. The temporal profiles were fit to an expression of the form, here given for the relaxation of OH($v = 1$)

$$[OH(v = 1)]_t = [OH(v = 1)]_0 \exp(-k_{v1}t)$$
$$+ \frac{k_{v2a}[OH(v = 2)]_0}{k_{v1} - k_{v2}} [\exp(-k_{v2}t) - \exp(-k_{v1}t)] \quad (1)$$

In this expression, $[OH(v = 1)]_t$ is the concentration of OH($v = 1$) at time t, while $[OH(v)]_0$ are initial concentrations in the specified vibrational states immediately after OH is formed by photolysis or by the reactions of O(^{1}D). k_{v1}' and k_{v2}' are the pseudo-first order rate coefficients (*i.e.*, the products of the bimolecular rate coefficients and the relaxer concentrations) for the relaxation of OH($v = 1$) and OH ($v = 2$), respectively; while k_{v2a}' is the rate coefficient for the specific relaxation of OH($v = 2$) into OH($v = 1$). The measured temporal profiles were fit to this form, with the assumption that $k_{v2a}' = k_{v2}'$. We made this assumption because k_{v2a}' and [OH($v = 2$)]$_0$ are not independent variables in the temporal expression; this assumption does not affect the measured values of the relaxation rate coefficients. The temporal profiles were fitted well by this expression. Analogous expressions are used when measuring the relaxation of OH ($v = 2$), with OH($v = 2$) and OH($v = 3$) replacing OH($v = 1$) and OH($v = 2$), respectively, and for the relaxation of OD ($v = 1$) and OD($v = 2$). Fig. 1 shows three examples of fitted temporal profiles for OH($v = 1$) being relaxed by approximately the same concentration of H$_2$O but with different photolytic sources of vibrationally excited OH.

HNO$_3$ photolysis at 248 nm produces little or no OH ($v > 2$). Thus, the above temporal expression is a correct representation of the kinetics of OH ($v = 1$) relaxation when this source of OH ($v = 1$) was used. However, the O(^{1}D) reactions we used generally produce significant amounts of OH($v > 2$) or OD($v > 2$)). Nevertheless, we found that this simplified two-state treatment of the temporal profiles led to rate coefficients for removal of OH($v = 1$) and OD($v = 1$) that were independent of the source of the vibrationally excited radicals. Generally, removal of vibrationally excited OH or OD becomes faster for higher vibrational states. Thus, the time scale for loss of OH($v > 2$) is shorter than that for the decay of OH($v = 1$), so that relaxation of OH ($v > 2$) has little impact on the measured rate coefficient for removal of OH($v = 1$).

To estimate the magnitude of the error which results from using this two-state approximation, we numerically modelled
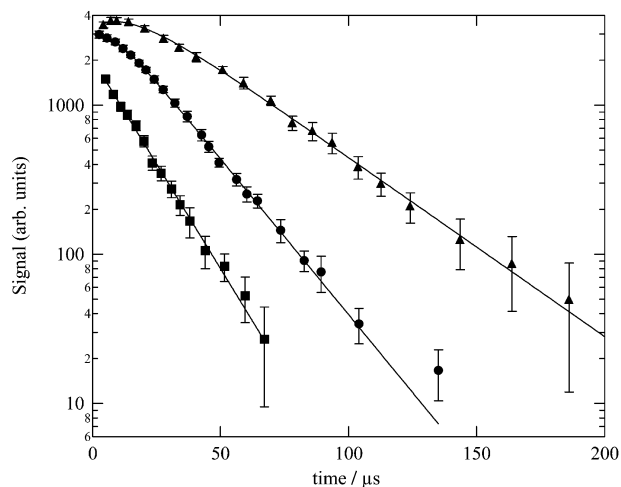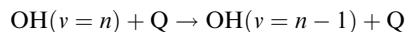
Fig. 1 Temporal profiles of PLIF signals from OH($v = 1$), produced using different photochemistries, during relaxation by *ca.* 2.5×10^{15} molecule cm^{-3} of H_2O at 296 K. Photolytic sources: triangles (▲), O(^{1}D) + H_2O ([O(^{1}D)]$_0$ = 6.7×10^{11} molecule cm^{-3}); circles (●), HNO_3 photolysis ([HNO_3] = 6.0×10^{14} molecule cm^{-3}); squares (■), H_2O_2 photolysis ([H_2O_2] = 6.5×10^{14} molecule cm^{-3}). The curvature at short times, due to relaxation from higher vibrational states of OH into ($v = 1$), is clear in the temporal profiles when O(^{1}D) + H_2O and HNO_3 photolysis are used as sources of OH($v = 1$). The lines are fits of the data to the expression on the right-hand side of (eqn (1)), except for the signals from OH($v = 1$), produced by H_2O_2 photolysis, which were fit to a single exponential function. The large differences in the pseudo-first order rate coefficients measured here are due to the relaxation of OH($v = 1$) by the photolytes.

several systems using a stepwise relaxation mechanism, where only one quantum of vibrational energy is lost per 'reaction'; that is,

$$OH(v = n) + Q \rightarrow OH(v = n - 1) + Q$$

As inputs for the model, we used yields for the vibrational states of OH (OD) from the O(^{1}D) reactions and rate coefficients for relaxation of OH (OD) from levels v = 1–4 at 298 K from the literature or estimated from our data. The literature sources, and details of the models and results, are given elsewhere.[30] The model results indicate that using the two-state approximation potentially results in errors of 10% or less for the rate coefficients for relaxation of OH ($v = 1$), but the errors could be as high as 20 and 30% for the relaxation of OD($v = 1$) by H_2O and D_2O, respectively. It is possible that vibrationally excited OH (OD) is removed by multi-quantum relaxation and, in the cases involving unlike isotopes, isotope-exchange reactions. If either process occurs, it will reduce the error due to the two-state approximation, because these processes would either decrease the amount of OH (OD) being relaxed into the state being monitored or would speed up the process of relaxing the higher states into the state being monitored.

At a given temperature, temporal profiles of the vibrationally excited radicals were recorded at a number of concentrations of the relaxing species (H_2O or D_2O). The fitted values of k_{v1}' from the above expression were then plotted against
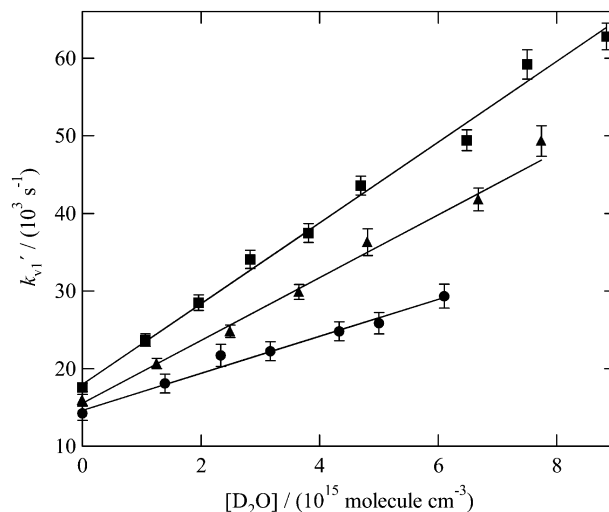

Fig. 2 Plots of k_{v1}' for OH ($v = 1$) relaxation by D_2O *versus* the concentration of D_2O at three temperatures: squares (■), 256 K; triangles (▲), 296 K; circles (●), 371 K. Error bars are the statistical uncertainty (2σ) from the fits of the temporal profiles. Lines are linear least-squares fits of these data and their slopes are the bimolecular rate coefficients k_{2a}. The large y-intercept is due to quenching of OH($v = 1$) by the photochemical precursors of OH($v = 1$).

the concentration of the relaxing species; the weighted linear least-squares fits for the slope of these plots are the bimolecular rate coefficients for the relaxation of OH($v = 1$) or OD($v = 1$). Fig. 2 shows examples of k_{v1}' for OH($v = 1$) plotted *versus* [D_2O] yielding values of k_{2a} at three different temperatures.

4. Experimental results

The rate coefficients for processes (1a) to (4b) at different temperatures are listed in Table 3, together with the photolytic sources of vibrationally excited OH (OD) and the concentrations of photolytes and relaxing species. We draw attention to the similarity of the values obtained for the relaxation of OH($v = 1$) by H_2O at 297 K using three different sources of the vibrationally excited radical. It is especially reassuring to note that the rate coefficient obtained using the reaction between O(^{1}D) atoms and H_2O agrees with those using photolysis of HNO_3 and H_2O_2, since cascading effects are likely to be most significant in the first case, and because reactions of O(^{1}D) are used to generate vibrationally excited OH (OD) in order to determine rate coefficients for the other isotopically related process (2a) to (4a).

The second-order rate coefficients reported in Table 3 are derived from plots of the first-order rate constants (k_{v1}'), derived from the analysis of the variation of LIF signals *versus* delay times, *versus* the concentrations of H_2O or D_2O included in the gas mixtures. The uncertainty of the weighted fits of k_{v1}' *versus* [H_2O] or [D_2O] was typically 2–10% (2σ). We estimate that uncertainties in the temperature of the bubbler used to control the concentration of H_2O (D_2O) and in measurement of the flows lead to an uncertainty of ±9% (2σ) for the concentration of H_2O (D_2O) in the LIF cell.

This journal is © the Owner Societies 2006

Phys. Chem. Chem. Phys., 2006, **8**, 4563–4574 | 4567

Table 3 Experimental conditions and measured rate coefficients ($k/10^{-12}$ cm^3 molecule^{-1} s^{-1})

Process	T/K	OH source	[HNO$_3$] or [H$_2$O$_2$]/ 10^{14} cm^{-3}	[H$_2$O]/10^{15} cm^{-3}	[D$_2$O]/10^{15} cm^{-3}	[O$_3$]/10^{11} cm^{-3}	[CH$_4$]/10^{16} cm^{-3}	[CD$_4$]/10^{15} cm^{-3}	$k \pm 2\sigma$
OH($v = 1$) + H$_2$O	263	HNO$_3$ + $h\nu$	8.8–17.9	0–6.43					13.9 ± 2.0
	296	O(^{1}D) + H$_2$O		2.27–16.8		24.3			12.3 ± 1.7
	297	HNO$_3$ + $h\nu$	5.2–7.9	0–9.54					11.7 ± 1.7
	297	H$_2$O$_2$ + $h\nu$	6.1–7.8	0–8.99					10.6 ± 1.6
	321	O(^{1}D) + H$_2$O		0.99–7.73		11.0			9.7 ± 1.4
	348	HNO$_3$ + $h\nu$	7.1–14.7	0–4.28					9.1 ± 1.7
	390	HNO$_3$ + $h\nu$	10.9–17.0	0–3.34					8.1 ± 1.4
OH($v = 1$) + D$_2$O	256	O(^{1}D) + CH$_4$			0–8.84	3.5	2.8		5.2 ± 0.7
	274	O(^{1}D) + CH$_4$			0–7.11	4.4	2.6		4.5 ± 0.8
	296	O(^{1}D) + CH$_4$			0–7.67	2.9	2.4		4.0 ± 0.7
	332	O(^{1}D) + CH$_4$			0–6.75	2.7	2.2		3.1 ± 0.5
	371	O(^{1}D) + CH$_4$			0–6.10	6.3	2.2		2.4 ± 0.4
OD($v = 1$) + H$_2$O	251	O(^{1}D) + CD$_4$		0–5.38		5.3		7.3	6.3 ± 0.8
	272	O(^{1}D) + CD$_4$		0–5.23		4.8		6.9	5.7 ± 0.6
	298	O(^{1}D) + CD$_4$		0–5.68		4.8		6.1	4.7 ± 0.5
	334	O(^{1}D) + CD$_4$		0–4.74		4.1		5.5	3.9 ± 0.4
	371	O(^{1}D) + CD$_4$		0–4.39		3.9		5.0	3.4 ± 0.4
OD($v = 1$) + D$_2$O	253	O(^{1}D) + D$_2$O			1.15–4.57	4.3			9.9 ± 1.6
	298	O(^{1}D) + D$_2$O			0.91–5.43	4.4			8.1 ± 1.0
	366	O(^{1}D) + D$_2$O			1.03–4.29	3.7			6.5 ± 0.8
OH($v = 2$) + D$_2$O	296	O(^{1}D) + CH$_4$			0–5.46	7.0	2.6		15.5 ± 3.3
OD($v = 2$) + H$_2$O	297	O(^{1}D) + CD$_4$		0–7.42		8.1		5.3	14.3 ± 1.7
OD($v = 2$) + D$_2$O	298	O(^{1}D) + D$_2$O			1.30–5.93	3.8			12.9 ± 1.6

The uncertainties listed for the rate coefficients in Table 3 are the sum (not in quadrature) of this uncertainty and the statistical error.

In Table 4, we compare the weighted average of the three values of k_{1a} that we have determined at *ca.* 298 K with rate coefficients for this process reported in the literature.[3,22,31] The agreement is very satisfactory, especially when account is taken of the fact that the values of k_{1a} and k_{1b} reported by Bradshaw *et al.*[31a] were derived from single kinetic traces. The small differences between the results from different studies are probably due to the difficulty of quantifying the concentrations of water vapour in our experiments and those of others.

The values of the rate coefficients listed in Table 4 for relaxation of OH($v = 1$) and OD($v = 1$) by H$_2$O and D$_2$O exhibit a clear, and moderately strong, *negative* dependence on temperature; that is, the rate coefficients increase as the temperature is lowered. We have matched the rate coefficients to two analytical expressions: (i) the Arrhenius equation $k(T) = A \exp(-E_{act}/RT)$, yielding a negative activation energy, and (ii) the form $k(T) = k(298) (T/298)^{-n}$. The fitting parameters are given in Table 5. Fig. 3, in which logarithmic values of the rate coefficients are plotted against the reciprocal of temperature, displays the quality of the fit to the Arrhenius expression. An equally good fit is obtained when

Table 4 Measured values of the rate coefficient for vibrational relaxation of OH($v = 1$), k_{1a}, and OH($v = 2$), k_{1b}, by H$_2$O at *ca.* 298 K

k_{1b}/cm^3 molecule^{-1} s^{-1}	k_{1a}/cm^3 molecule^{-1} s^{-1}	Method	[H$_2$O] measurement	Ref.
3.66 × 10^{-11}	2.09 × 10^{-11}	O$_3$ photolysis; O(^{1}D) + H$_2$O; LIF detection	185 nm absorption^a (σ = 7.2 × 10^{-20} cm^2)	22^a
2.58 × 10^{-11}	1.33 × 10^{-11}	Continuous OH from H + NO$_2$; OH ($v = 0$) excited to ($v = 2$) by IR radiation from Raman-shifted dye laser. LIF detection.	Capacitance hygrometer	31c
	1.36 × 10^{-11}	OH ($v = 1$) from flashlamp photolysis of HNO$_3$, LIF detection.	Manometric preparation of H$_2$O/Ar mixtures	3
7 × 10^{-11}	3 × 10^{-11}	O(^{1}D) + H$_2$O production of OH, LIF (Rate constant from one temporal profile).	Not reported	31a
	1.4 × 10^{-11}	Flow tube kinetics; OH ($v = 1$) directly from H + NO$_2$; EPR detection of OH.	Not reported	31b
	1.35 × 10^{-11}	Flow tube kinetics; OH ($v = 1$) directly from O + HBr; EPR detection of OH	Not reported	31d
	1.15 × 10^{-11}	See text	See text	This work

^{a} Only the rate coefficients based on $\sigma_{H_2O}^{184.9\ nm} = 7.2 \times 10^{-20}$ cm^2 are listed here.

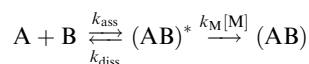**Table 5** Parameters describing temperature-dependence of rate coefficients

| Process | $k(T) = A e^{-E_a/RT}$ | | $k(T) = k(298)(T/298)^{-n}$ | |
	A^b	$E_a/R/K$	$k(298)^c$	n
$OH(v = 1) + H_2O$	24 ± 9	-460 ± 115	11.5 ± 0.5	1.47 ± 0.40
$OH(v = 1) + D_2O$	4.9 ± 1.6	-610 ± 90	3.85 ± 0.09	2.04 ± 0.19
$OD(v = 1) + H_2O$	9.2 ± 1.6	-485 ± 48	4.77 ± 0.08	1.63 ± 0.13
$OD(v = 1) + D_2O$	25.7 ± 0.9	-342 ± 10	8.18 ± 0.11	1.14 ± 0.09

^{a} Error bars are 2σ representations of the uncertainties of the fits. ^{b} Units are 10^{-13} cm^3 molecule^{-1} s^{-1}. ^{c} Units are 10^{-12} cm^3 molecule^{-1} s^{-1}.

the experimental data are fitted to the second, power law, expression. The error bars shown on the points in Fig. 3 represent only the statistical uncertainties.

5. Theoretical calculations

In order to examine further whether the relaxation of $OH(v = 1)$ and $OD(v = 1)$ by H_2O and D_2O might proceed *via* the formation of hydrogen-bonded complexes, we have adapted a method of Troe[32] that was originally designed to treat association reactions (*e.g.*, of A with B) in the limit of low pressure. The mechanism considered by Troe can be written:
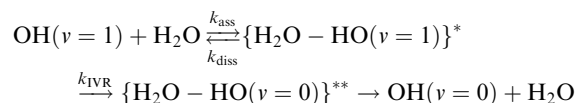
$$A + B \underset{k_{diss}}{\overset{k_{ass}}{\rightleftharpoons}} (AB)^* \overset{k_M[M]}{\longrightarrow} (AB)$$

Much of the methodology is given over to how one can estimate (k_{ass}/k_{diss}). This quantity may be viewed as a pseudo-equilibrium constant between the energised complexes formed in A + B collisions and separated A + B and is estimated using the methods of statistical mechanics. It is

Fig. 3 Values of the rate coefficients for relaxation of $OH(v = 1)$ and $OD(v = 1)$ by H_2O and D_2O: triangles (▲), k_{1a}; squares (■), k_{4a}; circles (●), k_{3a}; diamonds (◆), k_{2a}. The solid lines are the Arrhenius fits for each isotopic combination. The parameters yielded by these fits and those from fits to power dependences on temperature are given in Table 5.

assumed that $k_M[M] \ll k_{diss}$ and that $(AB)^*$ is in a steady-state concentration so that the second-order rate constant for association in the limit of low pressure is simply

$$k_{2nd}^\circ = (k_{ass}/k_{diss})k_M[M]$$

Our postulate is that vibrational relaxation *via* a collision complex can be treated in a similar manner, with $k_M[M]$ replaced by k_{IVR}; that is, the rate coefficient for transfer of the vibrational quantum originally present in the O–H (or O–D) vibration into the 'bath' of other modes in the complex. Thus, we represent the mechanism for the relaxation of $OH(v = 1)$ by H_2O with the scheme
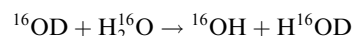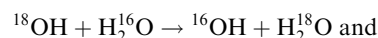
$$OH(v = 1) + H_2O \underset{k_{diss}}{\overset{k_{ass}}{\rightleftharpoons}} \{H_2O - HO(v = 1)\}^*$$

$$\overset{k_{IVR}}{\longrightarrow} \{H_2O - HO(v = 0)\}^{**} \rightarrow OH(v = 0) + H_2O$$

When $k_{IVR} \ll k_{diss}$,§ the second-order rate constant for vibrational relaxation (k_{relax}) is

$$k_{relax} = (k_{ass}/k_{diss})k_{IVR}$$

We proceed by using the Troe approach[32] to estimate (k_{ass}/k_{diss}) and then examine the values that k_{IVR} would have to have to yield the measured values of k_{relax}.

This mechanism does not explicitly include the possibility that an H (or D) atom exchange occurs. The thermal kinetics of this process have been investigated by Dubey *et al.*[33] by measuring rate constants for the isotopic scrambling reactions:

$$^{18}OH + H_2^{16}O \rightarrow {}^{16}OH + H_2^{18}O \text{ and}$$

$$^{16}OD + H_2^{16}O \rightarrow {}^{16}OH + H^{16}OD$$

At 300 K, they found rate constants of $(2.2 \pm 1.0) \times 10^{-16}$ and $(3 \pm 1.0) \times 10^{-16}$ cm^3 molecule^{-1} s^{-1}, respectively, for these two reactions, both four-to-five orders of magnitude smaller than those measured for the vibrational relaxation of $OH(v = 1)$ and $OD(v = 1)$ in the present work. As long as the energy originally in the OH (OD) vibrations remains localised in those vibrations, there is no reason to suppose that the rates of these reactions will be accelerated to anything like this extent by excitation of OH (or OD) to $v = 1$. Even when IVR has occurred in the H_2O–HO complex, arguments based on RRKM theory would suggest that it is far more likely that dissociation will occur to the original collision partners, rather

§ This appears to be a reasonable assumption, since the rate coefficient that Masgrau *et al.*[18d] estimate for the formation of H_2O–HO complexes is *ca.* 30 times greater than the rate coefficient for relaxation of $OH(v = 1)$ by H_2O.
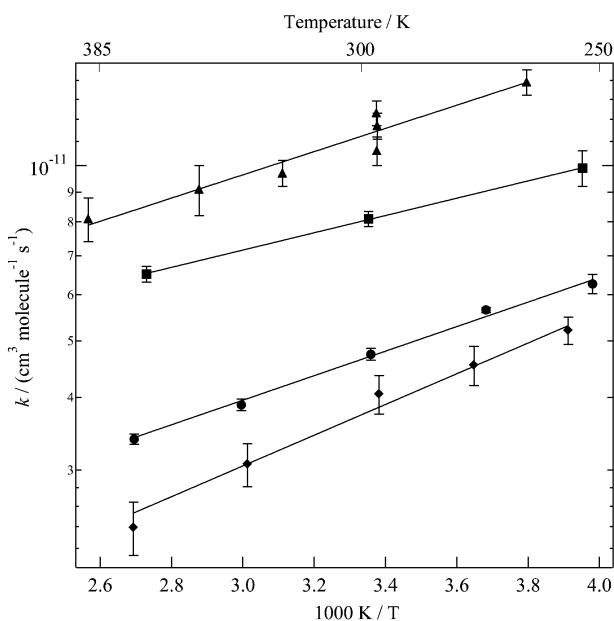
This journal is © the Owner Societies 2006

Phys. Chem. Chem. Phys., 2006, **8**, 4563–4574 | **4569**

Table 6 Frequencies (cm^{-1}), rotational constants (cm^{-1}) and energies (kJ mol^{-1}) for the H$_2$O–HO complex, its isotopomers and fragments at the CISD/cc-pVTZ level

Symmetry	H$_2$O–HO	H$_2$O–DO	D$_2$O–HO	D$_2$O–DO	Symmetry	H$_2$O	H$_2$O obs[b]	D$_2$O	OH	OH obs[b]	OD
A' [a]	140	137	105	104	A_1 [a]	1576	1595	1153	3562	3568	2593
A' [a]	174	172	171	169	A_1 [a]	3667	3657	2644			
A' [a]	415	304	412	299	B_2 [a]	3760	3756	2754			
A' [a]	1581	1581	1158	1158							
A' [a]	3537	2575	2671	2575							
A' [a]	3706	3706	3538	2671							
A' [a]	154	145	116	112							
A'' [a]	586	448	568	422							
A'' [a]	3799	3799	2784	2784							
B [c]	12.52	12.51	6.381	6.378		27.45		15.27	19.05		10.09
B [c]	0.2258	0.2256	0.2084	0.2072		14.77		7.392			
B [c]	0.2237	0.2227	0.2034	0.2023		9.603		4.980			
ZPE [d]	84.27	76.95	68.90	61.56		53.84		39.17	21.30		15.51
ΔZPE [d]	−9.14	−7.60	−8.43	−6.88							
$\Delta_r H_0$ [d]	−13.99	−15.52	−14.70	−16.24							
$H_{298.15}$–H$_0$ [d]	16.79	17.42	17.23	17.89		9.92		9.97	9.24		9.24
$\Delta_r H_{298.15}$ [d]	−16.36	−17.26	−16.68	−17.56							

[a] Frequencies, scaled by 0.9323, in cm^{-1}, see text. [b] From ref. 35. [c] Rotational constants in cm^{-1}. [d] In kJ mol^{-1}.

than over (or through, by tunnelling) the 40–50 kJ mol^{-1} barrier[18d] for the internal H-atom transfer and H (or D) atom scrambling. Finally, we point out that below we only treat the steps in the proposed mechanism up to the point that the IVR has occurred and the complex represented by {H$_2$O–HO(v = 0)}** has formed.

(a) *Ab initio* calculations on the hydrogen-bonded H$_2$O–HO system

In order to be able to estimate (k_{ass}/k_{diss}) for all four cases of relaxation that we have studied, using Troe's method, new *ab initio* calculations have been performed on the H$_2$O–HO system. First, the geometry of the lowest energy $^2A'$ state was obtained using configuration interaction theory with single and double excitations, as used by Xie and Schaefer,[18g] applied with the correlation-consistent triple zeta basis set of Dunning.[34] At this geometry, harmonic vibrational frequencies and rotational constants were calculated for H$_2$O–HO and its various isotopomers. Such calculations overestimate observed fundamental frequencies, largely because they neglect anharmonicity. Based on comparison with the fundamental frequencies of OH and H$_2$O, the present CISD/cc-pVTZ results were scaled by a factor of 0.9323, which reproduced the experimental values of the frequencies to within 20 cm^{-1}.[35] The scaled results for the complexes are given in Table 6. These calculations were carried out with the Gaussian 03 suite of programs.[36]

Next, an improved geometry was obtained using coupled cluster theory, with single, double and perturbatively-estimated triple excitations, with the augmented cc-pVTZ basis set.[34,37] The Molpro program suite was used to implement spin-unrestricted CCSD(T) theory based on a restricted Hartree–Fock wavefunction.[38] The T1 diagnostic was 0.009, which confirms the applicability of this correlated method based on a single-reference wavefunction.[39] The CCSD(T)/

aug-cc-pVTZ geometry is shown in Fig. 4. The energy at this geometry (and for OH and H$_2$O at their corresponding geometries) was evaluated with CCSD(T) theory with the basis set sequence aug-cc-pVDZ, aug-cc-pVTZ and aug-cc-pVQZ (see Table 7), which enables a systematic extrapolation of the energy, *via* an empirical exponential function, to the infinite or complete basis set (CBS) limit.[40] These energy differences were combined, along with corrections for spin–orbit splitting in OH and the complex (139 and 200 cm^{-1}, respectively[15,35]), and for changes in zero-point vibrational energy, to obtain the 0 K bond dissociation enthalpy $\Delta H_0 = D_0$ between the adduct and separated fragments. The binding enthalpy at 298.15 K, $\Delta_r H_{298.15}$, was obtained *via* enthalpy corrections based on the computed frequencies (assuming harmonic behaviour) and the experimental spin–orbit splittings noted above.

(b) Computational results

The CCSD(T) equilibrium geometry shown in Fig. 4 is very similar to that calculated by Ohshima *et al.*,[14] with a hydrogen bond length of 1.910 × 10^{-10} m. Our calculated bond length can also be compared with that obtained by Brauer *et al.*[15] *via* an analysis of their Fourier transform microwave spectrum, 1.952 × 10^{-10} m. The latter quantity should, of course, be
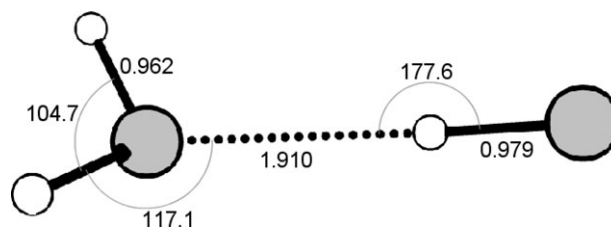

Fig. 4 Geometry of the lowest-lying $^2A'$ hydrogen-bonded complex between H$_2$O and OH computed at the CCSD(T)/aug-cc-pVTZ level.

Table 7 Energies calculated at the coupled cluster level[a]

Species	Aug-cc-pVDZ	Aug-cc-pVTZ	Aug-cc-pVQZ	CBS
OH	−75.584 019	−75.645 547	−75.664 444	−75.672 821
H_2O	−76.273 859	−76.342 326	−76.363 574	−76.373 136
H_2O–HO	−151.867 236	−151.997 256	−152.037 282	−152.055 084
ΔE/kJ mol^{-1} [b]	−24.57	−24.64	−24.32	−23.96

[a] RCCSD(T)/UHF energies obtained with different basis sets at the CCSD(T)/aug-cc-pVTZ geometry, and the extrapolation to the complete basis set limit, in au (1 au ≈ 2625.5 kJ mol^{-1}). [b] Energy difference between the H_2O-complex and the separated fragments H_2O + HO (excluding ZPE and spin–orbit corrections, see text).

larger because of vibrational averaging over the anharmonic stretching motion, and also because the very low lying A'' state, for which we compute a CCSD(T) hydrogen bond length of 1.938×10^{-10} m, may be significantly populated. The CBS extrapolation employed here eliminates any influence of basis set superposition error on the energy, which would lead to overestimated binding energies for theoretical methods based on moderate-sized basis sets. In fact the CCSD(T) dissociation energy with the three correlation consistent basis sets changed by less than about 1 kJ mol^{-1} (see Table 7), which indicates that good convergence has been achieved. As has been noted previously,[15] the angular momentum of the two spin–orbit states, $^2\Pi_{1/2}$ and $^2\Pi_{3/2}$, of OH persists in the adduct to yield the $^2A'$ ground state and a low-lying $^2A''$ state. The latter two are resolved as distinct states by standard non-relativistic computational methods, but the two states of OH are not. Consistent treatment of reactants and products, *i.e.*, correction of the energy of OH by half the spin–orbit splitting, lowers the calculated dissociation energy by *ca.* 0.8 kJ mol^{-1}. While small, this effect also contributes to previous values of D_0 falling higher than our best estimate of 14.0 kJ mol^{-1} (see Table 6). The contributions of electronic degeneracy to $H_{298}-H_0$ fortuitously cancel between reactants and adduct to within *ca.* 0.1 kJ mol^{-1}. Harmonic treatment of low-frequency modes is questionable, but with this simplification we derive $\Delta_r H_{298.15} = -16.4$ kJ mol^{-1}. This is at the positive end of previous estimates, but it appears to be the most reliable value to date.

(c) Estimates of the rates of relaxation

Troe's method[32] for estimating (k_{ass}/k_{diss}) proceeds in stages. First, one makes an initial estimate of this pseudo-equilibrium constant between A + B and AB* by calculating a density of harmonic vibrational states ($\rho_{vib,h}(E_0)$) for a rotationless (*i.e.*, $J = 0$) AB* energised complex at the dissociation energy (E_0) of AB (see eqn (4.4b) in ref. 32). The first two lines of each block of Table 8 lists values of $\rho_{vib,h}(E_0) kT$ and values of $(k_{ass}/k_{diss})_{E_0,J=0}$. In applying this method to estimating values of $(k_{ass}/k_{diss})_{E_0,J=0}$ for the four isotopically different cases, (1a), (2a), (3a) and (4a), of interest here, we have assumed that only the five low frequency modes in the complexes (see Table 6) are 'active'; that is, contribute to the density of vibrational states. The energies (E_0) at which we have calculated the harmonic density of states, *via* eqn (4.4b) in ref. 32, are those given as $-\Delta_r H_0$ in Table 6. It is noticeable that isotopic substitution changes the densities of harmonic vibrational states in the

complexes as one would expect as deuterium is substituted for hydrogen. However, as the values of $(k_{ass}/k_{diss})_{E_0, J=0}$ show, these changes are largely cancelled by corresponding changes in the partition functions of the 'reagents', OH (OD) and H_2O (D_2O).

Next, in Troe's prescription, one applies various corrections for factors omitted in the first estimate of (k_{ass}/k_{diss}): (a) anharmonicity (F_{anh}, see eqn (5.4) in ref. 32), (b) the spread of internal energies in AB* complexes formed in thermal collisions between A and B (F_E, see eqn (6.3) in ref. 32), and (c) the neglect of effects due to overall rotation (F_{rot}, see eqn (7.24) in ref. 32). These multiplicative factors all increase the estimates of (k_{ass}/k_{diss}) and yield the final estimates given in the third row of each block of Table 8. The measured rate constants for relaxation have then been divided by these results to obtain estimates of k_{IVR}.

A number of things are worthy of note: (i) for a given molecular system, the estimated values of k_{IVR} are reasonably independent of temperature, as one might expect; (ii) the observed temperature-dependences of k_{relax} are matched quite well by those of (k_{ass}/k_{diss}), giving some support to the hypothesis that relaxation in these cases is occurring *via* the

Table 8 Estimates of rate coefficients for intramolecular vibrational relaxation within the H_2O-complex and its isotopomers

	200 K	300 K	400 K
OH + H_2O			
$\rho_{vib,h}(E_0) kT$	72.7	109.0	145.3
$(k_{ass}/k_{diss})_{E_0,J=0}$/cm^3	5.2×10^{-23}	2.85×10^{-23}	1.85×10^{-23}
(k_{ass}/k_{diss})/cm^3	4.3×10^{-22}	1.72×10^{-22}	9.6×10^{-23}
$k_{relax}(v = 1)$/cm^3 s^{-1}	2.07×10^{-11}	1.14×10^{-11}	0.65×10^{-11}
k_{IVR}/s^{-1}	4.8×10^{10}	6.6×10^{10}	6.8×10^{10}
OH + D_2O			
$\rho_{vib,h}(E_0) kT$	139.7	209.6	279.4
$(k_{ass}/k_{diss})_{E_0,J=0}$/cm^3	5.9×10^{-23}	3.0×10^{-23}	1.93×10^{-23}
(k_{ass}/k_{diss})/cm^3	4.9×10^{-22}	1.82×10^{-22}	1.0×10^{-22}
$k_{relax}(v = 1)$/cm^3 s^{-1}	8.7×10^{-12}	3.8×10^{-12}	2.1×10^{-12}
k_{IVR}/s^{-1}	1.8×10^{10}	2.1×10^{10}	2.1×10^{10}
OD + H_2O			
$\rho_{vib,h}(E_0) kT$	149.5	224.3	299.1
$(k_{ass}/k_{diss})_{E_0,J=0}$/cm^3	5.0×10^{-23}	3.0×10^{-23}	1.97×10^{-23}
(k_{ass}/k_{diss})/cm^3	4.6×10^{-22}	1.64×10^{-22}	1.02×10^{-22}
$k_{relax}(v = 1)$/cm^3 s^{-1}	7.4×10^{-12}	4.7×10^{-12}	2.95×10^{-12}
k_{IVR}/s^{-1}	1.6×10^{10}	2.9×10^{10}	2.9×10^{10}
OD + D_2O			
$\rho_{vib,h}(E_0) kT$	287.7	431.6	575.5
$(k_{ass}/k_{diss})_{E_0,J=0}$/cm^3	5.8×10^{-23}	3.15×10^{-23}	2.1×10^{-23}
(k_{ass}/k_{diss})/cm^3	4.9×10^{-22}	1.94×10^{-22}	1.09×10^{-22}
$k_{relax}(v = 1)$/cm^3 s^{-1}	1.3×10^{-11}	8.1×10^{-12}	5.9×10^{-12}
k_{IVR}/s^{-1}	2.7×10^{10}	4.2×10^{10}	5.4×10^{10}

This journal is © the Owner Societies 2006

Phys. Chem. Chem. Phys., 2006, **8**, 4563–4574 | 4571

transient formation of hydrogen-bonded complexes; (iii) there are significant differences between the values of k_{IVR} for different molecular systems with those for the 'like-isotope' pairs, $OH + H_2O$ and $OD + D_2O$, being somewhat larger than those for the 'unlike-isotope' pairs, $OH + D_2O$ and $OD + H_2O$. These differences are discussed further in the next section.

6. Discussion and conclusions

Reactions of $O(^1D)$ were used to produce vibrationally excited OH and OD for all of the measurements on processes (2a, 2b), (3a, 3b) and (4a, 4b), and for two of the measurements on (1a). As discussed previously, when reactions of $O(^1D)$ are used to generate vibrationally excited OH (OD) significant errors may arise in the derived rate coefficients, because fits to the traces of LIF signals of $OH(v = 1)$ and $OD(v = 1)$ may be affected by OH and OD cascading down from higher levels into ($v = 1$). These effects have been estimated, via simple numeric modelling of the kinetics, to cause a potential error of ca. 8% when $O(^1D) + H_2O$ is employed to generate vibrationally excited OH. In this regard, the good agreement between the derived rate coefficients for relaxation of $OH(v = 1)$ by H_2O using different sources of vibrationally excited OH is reassuring. The potential errors for the rate coefficients for the relaxation of $OH(v = 1)$ by D_2O are similar.
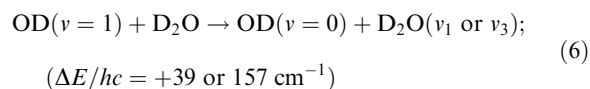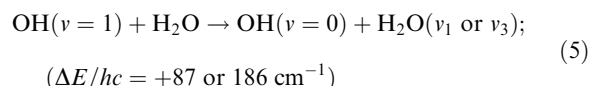
The errors in the rate coefficients for removal of $OD(v = 1)$ are larger than those for removal of $OH(v = 1)$ because reactions of $O(^1D)$ can produce OD in higher vibrational states, due to the closer spacing of the OD vibrational levels, and because the vibrational distribution of OD produced by these reactions is less well characterized than the vibrational distribution of OH produced by $O(^1D)$ reactions. In the case of $OH(v = 1) + D_2O$, the complication arising from 'cascading' is exacerbated because the corresponding rate coefficient for removal of $OD(v = 2)$ is only a factor of 1.6 larger than that for relaxation of $OD(v = 1)$. This makes the temporal profiles of $OD(v = 1)$ quite difficult to fit. Thus, our measured rate coefficients for removal of $OD(v = 1)$ by H_2O and D_2O have errors of up to 20 and 30%, respectively, due to this effect.

Next, we compare our results with those obtained, many years ago, on the relaxation of $HF(v = 1)$ by H_2O and D_2O. Unfortunately, only room temperature measurements are available for these systems and there are no data on the corresponding $DF(v = 1) + H_2O$, D_2O systems. For both $HF(v = 1) + H_2O$ and $HF(v = 1) + D_2O$, Hancock and Green[9] determined a relaxation rate coefficient of 1.25×10^{-10} cm^3 molecule^{-1} s^{-1} and the result for $HF(v = 1) + H_2O$ was supported by Frost et al.[11] who reported an identical value of the rate coefficient. A comparison between the vibrational relaxation of OH and HF is interesting because of the similarities between the two species. Thus, the $v = 1 \rightarrow v = 0$ vibrational transition energy in HF is equivalent to 3958.4 cm^{-1} (in OH it is 3569.6 cm^{-1}) and HF has a dipole moment of 1.826 D (OH: 1.668 D).[26] However, the dissociation energy of the hydrogen bond in H_2O–HF is given[41] as $D_e = 42.9$ kJ mol^{-1} and $D_0 = 34.3$ kJ mol^{-1}, values that are significantly larger than the corresponding quantities for H_2O–HO (see

Tables 1 and 6). It seems reasonable to suppose that relaxation in both these systems is facilitated by the transient formation of hydrogen-bonded complexes. However, the more strongly bound H_2O–HF complex probably survives long enough with respect to re-dissociation to $H_2O + HF(v = 1)$ to allow most of the complexes to undergo IVR with the result that the rate coefficient for relaxation is closer to that for formation of the complexes than in the case of $H_2O + OH(v = 1)$.

A second useful comparison is with our earlier results on the relaxation of $OH(v = 1)$ and $OD(v = 1)$ by HNO_3 and DNO_3.[12] Those previous results are similar to those reported in the present paper in three respects. Firstly, the rate coefficients at 298 K for the relaxation of $OH(v = 1)$ by HNO_3, of $OH(v = 1)$ by DNO_3, of $OD(v = 1)$ by HNO_3 and $OD(v = 1)$ by DNO_3 are factors of 2.0, 1.5, 1.6 and 2.2 larger than those shown in Table 5 for the corresponding relaxation process in the $OH(v = 1)$, $OD(v = 1) + H_2O$, D_2O system. Secondly, as the numbers in the previous sentence indicate, the relative values of the rate coefficients for different isotopic pairs are rather similar. Thirdly, the temperature dependences of the two sets of rate constants are also similar. Thus, the values of the parameter n given in the last column of Table 5 (1.47, 2.04, 1.63 and 1.14) can be compared with those of 1.8, 2.6, 2.4 and 2.2 for the relaxation of $OH(v = 1)$ by HNO_3, of $OH(v = 1)$ by DNO_3, of $OD(v = 1)$ by HNO_3 and of $OD(v = 1)$ by DNO_3, respectively.

We have argued in the previous section that the large values of the rate coefficients for relaxation of $OH(v = 1)$ and $OD(v = 1)$ in collisions with H_2O and D_2O and the rather strong negative dependence of these rate coefficients on temperature are at the very least consistent with relaxation via transient hydrogen-bonded complexes, such as H_2O–HO. In the two cases of $OH(v = 1) + H_2O$ and $OD(v = 1) + D_2O$, it is possible that vibrational relaxation occurs, without the formation of weakly-bound complexes, by near-resonant vibration–vibration (V–V) energy exchange in direct collisions; that is,

$$OH(v = 1) + H_2O \rightarrow OH(v = 0) + H_2O(v_1 \text{ or } v_3);$$
$$(\Delta E/hc = +87 \text{ or } 186 \text{ cm}^{-1}) \tag{5}$$

$$OD(v = 1) + D_2O \rightarrow OD(v = 0) + D_2O(v_1 \text{ or } v_3);$$
$$(\Delta E/hc = +39 \text{ or } 157 \text{ cm}^{-1}) \tag{6}$$

However, for $OH(v = 1) + D_2O$ and $OD(v = 1) + H_2O$, any vibrational exchange channels involving single quantum transitions in D_2O and H_2O are far from resonant and, in the second case, also strongly endothermic. Given that relaxation remains rapid even in these cases, it seems that relaxation via hydrogen-bonded complexes is the most likely mechanism in all four cases. This is consistent with the similarity of the temperature-dependence for all four processes which, in the Troe-type calculations that we have presented, is attributable to the temperature-dependence of the factor (k_{ass}/k_{diss}) and depends, in turn, on the strong dependence of k_{diss} on the internal energy of the complex. If V–V energy exchange in direct collisions was contributing significantly to the relaxation in processes (1a) and (4a), we would expect their rate

coefficients to have a noticeably smaller temperature-dependence than those for the slower, non-resonant processes (2a) and (3a). This is not what we observe.

At *ca.* 298 K, the rate constants for relaxation of OH($v = 2$) by D_2O, of OD($v = 2$) by H_2O and of OD($v = 2$) by D_2O (see Table 3) are factors of *ca.* 3.9, 3.0 and 1.6, respectively, larger than the corresponding rate coefficients for relaxation of OH($v = 1$) and OD($v = 1$). This acceleration probably reflects a faster rate of IVR as a result of the increased excitation and anharmonicity in the OH (OD) vibration.

The calculations presented in the previous section suggest that, although the rates of IVR are similar in all the isotopically different systems that we have studied, k_{IVR} for H_2O–HO ($v = 1$) > k_{IVR} for D_2O–DO($v = 1$) > k_{IVR} for H_2O–DO ($v = 1$) ≈ k_{IVR} for D_2O–HO($v = 1$). This ordering indicates that IVR is (slightly) favoured in isotopically 'non-mixed' systems, an effect that may reflect the possibility of near-resonant vibrational energy exchange within the H_2O–HO ($v = 1$) and D_2O–DO($v = 1$) complexes. Alternatively, it might result from some participation of the direct near-resonant V–V processes represented by processes (5) and (6).

The only direct measurements of IVR rates in complexes involving OH($v > 0$) are those of Lester and her co-workers.[42–44] They generate weakly bound complexes in low temperature jet expansions and perform vibrational action spectroscopy to characterise the structure and dynamics of these species. They have not carried out experiments on the hydrogen-bonded complexes formed between OH radicals and H_2O. The only hydrogen-bonded complexes whose dynamics they have investigated are those formed between OH and CO[42] (and OD + OC)[43] and OH and C_2H_2.[44] Their experiments can measure vibrational predissociation lifetimes <0.15 ns, from observations of spectroscopic linewidths, or >5 ns from direct time-domain measurements. It appears that the time scale for the overall decay of the OH($v = 2$)–OC complexes[42b] lies between these values. In comparing IVR rates inferred from our experiments and those determined from Lester's experiments one should bear in mind that the complexes in her group's experiments are internally 'cold', apart from the specific excitation of the OH (OD) stretch, whereas the complexes formed in collisions, as in our experiments, will have energy released into the low frequency vibrational modes of the complex as a consequence of the formation of the hydrogen bond.

To summarise, we have measured rate coefficients for the vibrational relaxation of OH($v = 1$) and OD($v = 1$) by H_2O and D_2O at temperatures between 251 and 390 K, and for the vibrational relaxation of OH($v = 2$) by D_2O and OD($v = 2$) by H_2O and D_2O at *ca.* 298 K. On the bases of the magnitude of the rate coefficients for relaxation of OH($v = 1$) and OD($v = 1$) and their temperature-dependence, we propose that relaxation involves the transient formation of hydrogen-bonded complexes which can undergo intramolecular vibrational redistribution at a rate competitive with their re-dissociation. We have modelled this process for the isotopically different systems using the results of new *ab initio* calculations and a method, due to Troe, for treating processes that proceed *via* complex formation. These calculations suggest that the measured rates of relaxation will be reproduced if the rate coefficients for IVR range from *ca.* 8×10^{10} s^{-1} in the H_2O–HO($v = 1$) complex to *ca.* 2×10^{10} s^{-1} in the D_2O–HO($v = 1$) complex.

References

1 J. T. Yardley, *Introduction to Molecular Energy Transfer*, Academic Press, New York, 1980.
2 (*a*) K. Glänzer and J. Troe, *J. Chem. Phys.*, 1975, **63**, 4352; (*b*) M. Quack and J. Troe, *Ber. Bunsen-Ges. Phys. Chem.*, 1977, **81**, 160; (*c*) R. P. Fernando and I. W. M. Smith, *Chem. Phys. Lett.*, 1979, **66**, 218; (*d*) R. P. Fernando and I. W. M. Smith, *J. Chem. Soc., Faraday Trans. 2*, 1981, **77**, 459.
3 I. W. M. Smith and M. D. Williams, *J. Chem. Soc., Faraday Trans. 2*, 1985, **81**, 1849.
4 L. D'Ottone, D. Bauer, P. Campuzano-Jost, M. Fardy and A. J. Hynes, *Faraday Discuss.*, 2005, **130**, 111.
5 J. Brunning, D. W. Derbyshire, I. W. M. Smith and M. D. Williams, *J. Chem. Soc., Faraday Trans. 2*, 1988, **84**, 105.
6 M. A. Blitz, K. J. Hughes and M. J. Pilling, *J. Phys. Chem. A*, 2003, **107**, 1971.
7 I. W. M. Smith, *J. Chem. Soc., Faraday Trans.*, 1997, **93**, 3741.
8 (*a*) J. F. Bott and N. Cohen, *J. Chem. Phys.*, 1973, **58**, 4539; (*b*) J. F. Bott and N. Cohen, *J. Chem. Phys.*, 1974, **61**, 681.
9 J. K. Hancock and W. H. Green, *J. Chem. Phys.*, 1972, **57**, 4515.
10 J. A. Blauer, W. C. Solomon, L. H. Sentman and T. W. Owen, *J. Chem. Phys.*, 1972, **57**, 3277.
11 R. J. Frost, D. S. Green, M. K. Osborn and I. W. M. Smith, *Int. J. Chem. Kinet.*, 1986, **18**, 885.
12 D. C. McCabe, S. S. Brown, M. K. Gilles, R. K. Talukdar, I. W. M. Smith and A. R. Ravishankara, *J. Phys. Chem. A*, 2003, **107**, 7762.
13 S. S. Brown, J. B. Burkholder, R. K. Talukdar and A. R. Ravishankara, *J. Phys. Chem. A*, 2001, **105**, 1605.
14 Y. Ohshima, K. Sato, Y. Sumiyoshi and Y. Endo, *J. Am. Chem. Soc.*, 2005, **127**, 1108.
15 C. S Brauer, G. Sedo, E. M. Grumstrup, K. R. Leopold, M. D. Marshall and H. O. Leung, *Chem. Phys. Lett.*, 2005, **401**, 420.
16 (*a*) V. S. Langford, A. J. McKinley and T. I. Quickenden, *J. Am. Chem. Soc.*, 2000, **122**, 12859; (*b*) P. D. Cooper, H. G. Kjaergaard, V. S. Langford, A. J. McKinley, T. I. Quickenden and D. P. Schofield, *J. Am. Chem. Soc.*, 2003, **125**, 6048.
17 (*a*) H. J. Deyerl, A. K. Luong, T. G. Clements and R. E. Continetti, *Faraday Discuss.*, 2000, **115**, 147; (*b*) D. W. Arnold, C. Xu and D. M. Neumark, *J. Chem. Phys.*, 1995, **102**, 6088.
18 (*a*) H. Basch and S. Hoz, *J. Phys. Chem. A*, 1997, **101**, 4416; (*b*) M. R. Hand, C. F. Rodriquez, I. H. Williams and G. G. Balint-Kurti, *J. Phys. Chem. A*, 1998, **102**, 5958; (*c*) K. S. Kim, H. S. Kim, J. H. Jang, B. J. Mhin, Y. M. Xie and H. F. Schaefer, *J. Chem. Phys.*, 1991, **94**, 2057; (*d*) L. Masgrau, A. Gonzalez-Lafont and J. M. Lluch, *J. Phys. Chem. A*, 1999, **103**, 1044; (*e*) T. Uchimaru, A. K. Chandra, S. Tsuzuki, M. Sugie and A. Sekiya, *J. Comput. Chem.*, 2003, **24**, 1538; (*f*) B. Wang, H. Hou and Y. Gu, *Chem. Phys. Lett.*, 1999, **303**, 96; (*g*) Y. Xie and H. F. Schaefer, *J. Chem. Phys.*, 1993, **98**, 8829; (*h*) Z. Zhou, Y. Qu, A. Fu, B. Du, F. He and H. Gao, *Int. J. Quantum Chem.*, 2002, **89**, 550.
19 S. Aloisio and J. S. Francisco, *Acc. Chem. Res.*, 2000, **33**, 825.
20 G. L. Vaghjiani and A. R. Ravishankara, *J. Phys. Chem.*, 1989, **93**, 1948.
21 G. Ondrey, N. van Veen and R. Bersohn, *J. Chem. Phys.*, 1983, **78**, 3732.

This journal is © the Owner Societies 2006

Phys. Chem. Chem. Phys., 2006, **8**, 4563–4574 | 4573

22 E. Silvente, R. C. Richter and A. J. Hynes, *J. Chem. Soc., Faraday Trans.*, 1997, **93**, 2821.
23 (*a*) K.-H. Gericke, F. J. Comes and R. D. Levine, *J. Chem. Phys.*, 1981, **74**, 6106; (*b*) C. B. Cleveland and J. R. Wiesenfeld, *J. Chem. Phys.*, 1992, **96**, 248.
24 (*a*) P. M. Aker, J. J. A. O'Brien and J. J. Sloan, *J. Chem. Phys.*, 1986, **84**, 745; (*b*) S. G. Cheskis, A. A. Iogansen, P. V. Kulakov, I. Y. Razuvaev, O. M. Sarkisov and A. A. Titov, *Chem. Phys. Lett.*, 1989, **155**, 37; (*c*) C. R. Park and J. R. Wiesenfeld, *J. Chem. Phys.*, 1991, **95**, 8166.
25 W. A. Guillory, K. H. Gericke and F. J. Comes, *J. Chem. Phys.*, 1983, **78**, 5993.
26 *CRC Handbook of Chemistry and Physics*, CRC Press, Boca Raton, FL, 1989.
27 A. H. Harvey and E. W. Lemmon, *J. Phys. Chem. Ref. Data*, 2002, **31**, 173.
28 W. Wagner, A. Saul and A. Pruss, *J. Phys. Chem. Ref. Data*, 1994, **23**, 515.
29 W. A. Van Hook, *J. Phys. Chem.*, 1968, **72**, 1234.
30 D. C. McCabe, PhD thesis, University of Colorado, Boulder, 2004.
31 (*a*) J. D. Bradshaw, M. O. Rodgers and D. D. Davis, *Appl. Opt.*, 1984, **23**, 2134; (*b*) G. P. Glass, H. Endo and B. K. Chaturvedi, *J. Chem. Phys.*, 1982, **77**, 5450; (*c*) G. A. Raiche, J. B. Jeffries, K. J. Rensberger and D. R. Crosley, *J. Chem. Phys.*, 1990, **92**, 7258; (*d*) J. E. Spencer and G. P. Glass, *Int. J. Chem. Kinet.*, 1977, **9**, 97.
32 J. Troe, *J. Chem. Phys.*, 1977, **66**, 4758.
33 M. K. Dubey, R. Mohrschladt, N. M. Donahue and J. G. Anderson, *J. Phys. Chem. A*, 1997, **101**, 1494.
34 T. H. Dunning Jr, *J. Chem. Phys.*, 1989, **90**, 1007.
35 *NIST-JANAF Thermochemical Tables*, ed. M. W. Chase, Jr., American Chemical Society and the American Institute of Physics, Woodbury, NY, 1998.
36 M. J. Frisch, G. W. Trucks, H. B. Schlegel, G. E. Scuseria, M. A. Robb, J. R. Cheeseman, J. J. A. Montgomery, T. Vreven, K. N. Kudin, J. C. Burant, J. M. Millam, S. S. Iyengar, J. Tomasi, V. Barone, B. Mennucci, M. Cossi, G. Scalmani, N. Rega, G. A. Petersson, H. Nakatsuji, M. Hada, M. Ehara, K. Toyota, R. Fukuda, J. Hasegawa, M. Ishida, T. Nakajima, Y. Honda, O. Kitao, H. Nakai, M. Klene, X. Li, J. E. Knox, H. P. Hratchian, J. B. Cross, C. Adamo, J. Jaramillo, R. Gomperts, R. E. Stratmann, O. Yazyev, A. J. Austin, R. Cammi, C. Pomelli, J. W. Ochterski, P. Y. Ayala, K. Morokuma, G. A. Voth, P. Salvador, J. J. Dannenberg, V. G. Zakrzewski, S. Dapprich, A. D. Daniels, M. C. Strain, O. Farkas, D. K. Malick, A. D. Rabuck, K. Raghavachari, J. B. Foresman, J. V. Ortiz, Q. Cui, A. G. Baboul, S. Clifford, J. Cioslowski, B. B. Stefanov, G. Liu, A. Liashenko, P. Piskorz, I. Komaromi, R. L. Martin, D. J. Fox, T. Keith, M. A. Al-Laham, C. Y. Peng, A. Nanayakkara, M. Challacombe, P. M. W. Gill, B. Johnson, W. Chen, M. W. Wong, C. Gonzalez and J. A. Pople, *GAUSSIAN 03*, Gaussian, Wallingford, CT, version C.02, 2004.
37 R. A. Kendall, T. H. Dunning, Jr and R. J. Harrison, *J. Chem. Phys.*, 1992, **96**, 6796.
38 H.-J. Werner, P. J. Knowles, R. Lindh, M. Schütz, P. Celani, T. Korona, F. R. Manby, G. Rauhut, R. D. Amos, A. Bernhardsson, A. Berning, D. L. Cooper, M. J. O. Deegan, A. J. Dobbyn, F. Eckert, C. Hampel, G. Hetzer, A. W. Lloyd, S. J. McNicholas, W. Meyer, M. E. Mura, A. Nicklaß, P. Palmieri, R. Pitzer, U. Schumann, H. Stoll, A. J. Stone, R. Tarroni and T. Thorsteinsson, *Molpro Quantum Chemistry Package*, Birmingham, UK, version 2002.6, 2003.
39 T. J. Lee and P. R. Taylor, *Int. J. Quantum Chem.*, 1989, **S23**, 199.
40 J. M. L. Martin, in *Computational Thermochemistry*, ed. K. K. Irikura and D. J. Frurip, American Chemical Society, Washington, DC, 1998, American Chemical Society Symp. Ser. 677, ch. 12.
41 (*a*) A. C. Legon, D. J. Millen and H. M. North, *Chem. Phys. Lett.*, 1987, **135**, 303; (*b*) A. C. Legon and D. J. Millen, *Chem. Soc. Rev.*, 1992, **21**, 71.
42 (*a*) M. D. Marshall, B. V. Pond and M. I. Lester, *J. Chem. Phys.*, 2003, **118**, 1196; (*b*) B. V. Pond and M. I. Lester, *J. Chem. Phys.*, 2003, **118**, 2223.
43 I. B. Pollack, M. Tsiouris, H. O. Leung and M. I. Lester, *J. Chem. Phys.*, 2003, **119**, 118.
44 J. B. Davey, M. E. Greenslade, M. D. Marshall, M. I. Lester and M. D. Wheeler, *J. Chem. Phys.*, 2004, **121**, 3009.

4574 | *Phys. Chem. Chem. Phys.*, 2006, **8**, 4563–4574

This journal is © the Owner Societies 2006